Finite-Element Analysis of Ring Gear/Casing Spline Contact

S. Sundararajan* and S. Amin†
Pratt & Whitney Canada, Longueuil, Quebec, J4K 4X9 Canada

The speed reduction from turbine to propeller is achieved in the Pratt and Whitney PT6 turbo propeller engines through a two-stage epicyclic gear train. In this arrangement, the ring gear is locked to the casing through external splines. The orbitting of the planet gears generate cyclic stresses in the teeth fillets of the ring gear and the casing. The sliding contact between the steel ring gear and the casing splines generates wear. A two-dimensional finite-element computer program was extended to iteratively solve the problem of load-dependent contact between the splines. Using this program, the nonuniform distribution of the reactive load and the relative sliding on the loaded splines are calculated for any planet gear load position. The analysis predicts that the relative sliding reduces through a change in the spline pressure angle from 20–30 deg. Spline wear is practically eliminated in field engine gearboxes through this design change. The cyclic variation of the fillet stresses are also determined due to the orbitting planet load using a detailed network and by imposing boundary displacements. Qualitative comparison of the stress prediction is made using instrumented test results. The paper demonstrates the analysis procedure using a typical ring gear and casing combination.

Nomenclature

D_{IJ}	=	distance between nodes, I and J
d	=	relative sliding between the splines
I, J, K	=	probable contact node triplet
FN	=	normal load on the spline
F_R	=	radial component of the planet load
F_θ	=	tangential component of the planet load
N	=	vector normal to line joining nodes I and J
rpm	=	rotational speed of the planet carrier
SHP	=	Shaft horse power of the engine
S_K	=	distance between I node and the projection of K node on line I-J
U_I, U_J, U_K	=	X displacements of nodes I, J, and K
V_I, V_J, V_K	=	Y displacements of nodes I, J, and K
Λ, *Mue*	=	direction cosines of the vector N
δN_0	=	shortest distance between K node and the line I-J
ϕ	=	pressure angle of the splines

Introduction

PLANETARY gearboxes have been shown to offer the most reliable and compact way of achieving the speed reduction between the turbine and the propeller in the PT6 turbo propeller engines. The engines are produced in power levels ranging from 475–1424 SHP. The design of these gearboxes as well as those in other engine models were optimized through extensive use of the finite-element method (see, e.g., Refs. 1 and 2). The improved understanding of the behavior of the gear components through the use of this method is also demonstrated in Refs. 3 and 4. It is important to analyze gear components as structures rather than as cantilevered teeth. The finite-element method offers a convenient means of taking into account the effect of the spatial variation of the stiffness on the stresses in the gear elements. The load-dependent contact between the gear components makes the problem nonlinear and necessitates the use of specialized computer programs. One such computer program was prepared and used successfully for a detailed analysis of the contact between the ring gear and the casing.

Presented as Paper 88-2981 at AIAA/ASME/SAE/ASEE 24th Joint Propulsion Conference, Boston, MA, July 11–13, 1988; received March 8, 1989; revision received Oct. 21, 1989; accepted for publication Oct. 27, 1989.

*Chief, Turboprop Compressor Structures.
†Staff Engineer, Turbofau Static Structures.

Contact Analysis Method

A detailed description of the iterative contact analysis procedure based on the finite-element method is presented in Ref. 1. For the sake of completeness, the method is summarized here. Basically, the problem involves the determination of the contacting portions of the boundaries of the structures and the resulting displacement constraints for any particular load application. Two conditions should thus be satisfied: 1) the contacting boundaries should slide without crossing each other, and 2) there should be no tensile reactions on the portions of the boundaries in contact. The distribution of stiffness in the contacting structures plays a major role in arriving at the final deformed shape and the resulting stresses. The finite-element method offers an excellent means of computing and taking into account the effect of the stiffness distribution.

The basic steps in the analysis are as follows:

1) Supply minimum connecting boundary conditions between the structures where the contact is going to be most definite for the applied loads.

2) Find the deformed portions of the structures as well as the reactions at the assumed contacting nodes.

3) Supply sliding boundary conditions where the structure nodes have crossed and remove previously assumed connections if there are tensile reactions present.

4) Go to step 2 and so on until contacting structures are not crossing each other and the contact reactions are not tensile.

The sliding boundary conditions between the sets of three nodes—the node (K) belonging to one structure that crosses two nearest nodes (J and I) belonging to the other contacting structure—can be derived. The K, J, I nodes should be positioned such that they form a clockwise set for the X-Y axis system indicated below along with the functional form of the boundary condition:

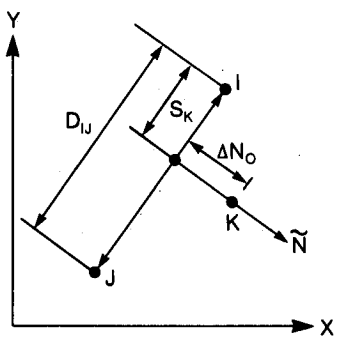

$$U_K = -\frac{\mu}{\lambda} V_K + \left\{ I - \frac{(S_K)}{(D_{IJ})} \right\} U_I + \frac{\mu}{\lambda} \left\{ I - \frac{(S_K)}{D_{IJ}} \right\} U_I + \frac{(S_K)}{D_{IJ}} U_J + \frac{\mu}{\lambda} \frac{(S_K)}{D_{IJ}} V_J - \frac{\Delta N_0}{\lambda}$$

If $\lambda = O$

$$V_K = \left\{ I - \frac{(S_K)}{(D_{IJ})} \right\} (V_I) + \frac{(S_K)}{D_{IJ}} V_J - \frac{\Delta N_0}{\mu}$$

Using the basic procedure explained above, a two-dimensional computer program was prepared with linear strain triangular elements. Several extensions were added such as the restart option to analyze a number of load cases, performing the iterations on a limited number of probable contacting nodes to save computing time and the inclusion of frictional contact. Frictional contact is analyzed by applying the frictional force at the compressive reaction nodes before proceeding to step 4 above. This should be applied as an opposing force pair on the ring gear and the casing against the directions of motion in the last iteration. A successful application of the computer program to resolve field problems in planetary gearbox casing splines is explained in the following sections.

Epicyclic Gear Stage Geometry

In the PT6 turbopropeller engines, the turbine-to-propeller speed reduction is obtained using a two-stage planetary gearbox. Figure 1 shows the front view of a typical first stage in the speed-reduction gear train system. The number of planets are typically three in the first stage and five in the second stage. Each stage incorporates a floating sun gear, orbitting planet gears assembled in a rotating planet carrier, and a "fixed" ring gear. The external splines of the ring gear are locked against rotation by the intermeshing internal splines of the casing. The high speed and low torque at the sun gear are transformed into reduced speed and increased torque at the planet carrier. The gears are made of low carbon steel, AMS6265, which is case carburized for high surface hardness on the gear teeth faces and fillets. The casing is made of magnesium alloy, AMS4439. The casing spline contacting faces are hardened in some engine models using a process called "magnadising."

Structural Analysis of Ring Gear/Casing Assembly

The radial and tangential loads from the planet on the internal teeth of the ring gear are reacted by the splines of the casing. The ring gear is thus subjected to a net radial load and torsional moment around each planet position. The deflection of the ring gear causes the spline reaction to be concentrated in a few splines. There will be relative sliding between the splines of the ring gear and the casing involved in the torque transfer. The fillets of the gear teeth and the splines are also subjected to high stresses. The relative sliding at the splines as well as the stresses in the fillets vary cyclically as the planets orbit. This gives rise to high cycle fatigue conditions with the tooth fillets registering five stress cycles per revolution of the planet carrier in the five-planet configuration. The framework of the structural analysis thus reduces to the calculation of the contact loads and the sliding between the steel and the magnesium splines as well as the fillet stress variations.

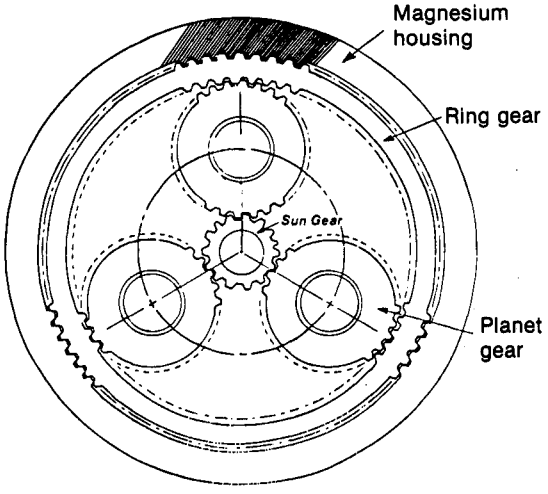

Fig. 1 Typical epicyclic system (stage 1).

Spline Contact Analysis

The distribution of spline reaction due to the planet load can be determined using the contact analysis program described earlier. The calculation of the orbitting planet load in a five-planet design for a shaft horsepower of 1120, planet carrier speed of 1210 rpm, planet orbitting diameter of 8.5 in., and planet gear tooth pressure angle of 27 deg is shown in Fig. 2 and calculated as follows:

Planet carrier torque	=	SHP*63025/rpm = 58400 lb in.
Planet gear bore reaction	=	58400/(5*(8.5/2)) = 2748 lb per planet
Tangential orbitting load	=	2748/2 = 1374 lb per planet
Radial orbitting load	=	1374*tan(27) = 700 lb per planet

The finite-element model required will be a 72-deg segment of the ring gear and the casing assembly using the periodic symmetry of a five-planet arrangement. Care should be taken in defining the coordinates of the finite-element nodes on the contacting faces of the ring gear and casing splines. This is because the calculated spline load distribution is sensitive to the initial clearance conditions between the spline pairs. The planet load is typically applied at the pitch location of the ring gear internal tooth. Figure 3 shows an example of the generated network. The modeling effort is greatly simplified using a dedicated preprocessor that requires as input only the gear and spline data and the casing outer diameter.

The outer surface of the casing is fixed radially and tangentially, and symmetry conditions are applied to the periodic boundaries of the ring gear and casing segment. At a partic-

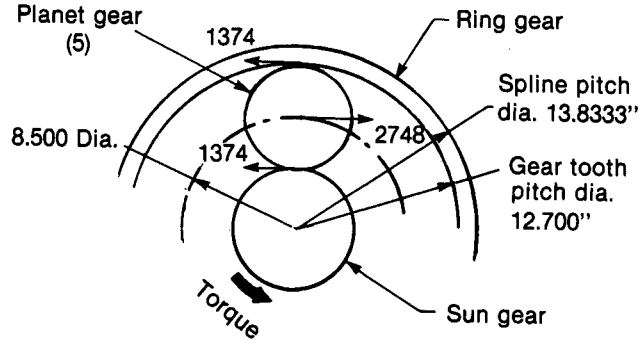

Fig. 2 Schematic for gear load calculations.

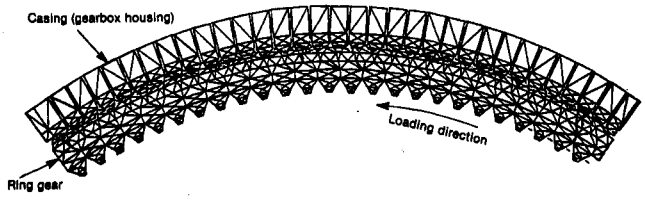

Fig. 3 Finite-element model for spline contact analysis.

ular planet load position, contact boundaries have to be manually given between the nodes of one spline pair that is definitely going to be in contact. The functional boundary condition should be according to the equation given in the earlier section. The iterative contact analysis is then performed by the computer program to determine the remaining contacting splines. The reactions at the finite-element nodes of the splines give the spline load distribution while the nodal displacements are used to calculate the relative sliding for the planet position examined. Figure 4 shows sample results for

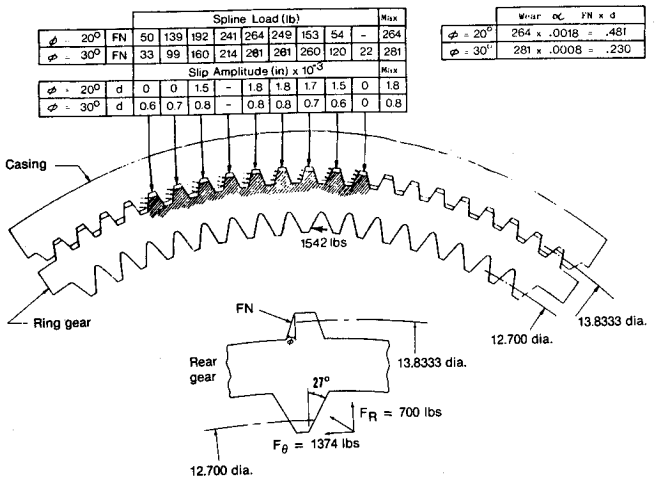

Fig. 4 Spline loads and relative sliding.

two designs with different values of spline pressure angle. The analysis is repeated for different planet load positions in one run using the multiload option in the program.

Fillet Stress Variation

The critical fillets are those of the ring gear internal teeth and the splines of the ring gear and casing. All of the casing spline fillets can be assumed to register equal stress variations due to the orbitting planet loads. However, since the number of splines is not equal to the number of internal teeth, the ring gear radial thickness is not constant and hence some fillets of the ring gear will register larger stress variations than the others. Specifically, the fillets of the ring gear internal teeth and splines in approximately the same tangential position would be more critical. The estimation of these stresses and their variations require a detailed network. Figure 5 shows such a network for a portion of the coarse grid shown in Fig. 4 used for the spline contact analysis. Boundary displacements obtained from the spline contact analysis and loads on the ring gear internal tooth node (if present) are specified and the critical stresses are calculated for each planet position. Figure 5 also shows sample distribution of stresses in the fillets of the ring gear and casing. The fillet stress-analysis calculations are performed for different planet positions to obtain the stress variations needed for the high cycle fatigue evaluation. A sample plot of these stress variations is shown in Fig. 6. It should be noted that the network is refined in one tooth location only and the peak stresses are computed for this location. The analysis is performed for twenty-five (number of ring gear teeth in the 72-deg segment) positions of the

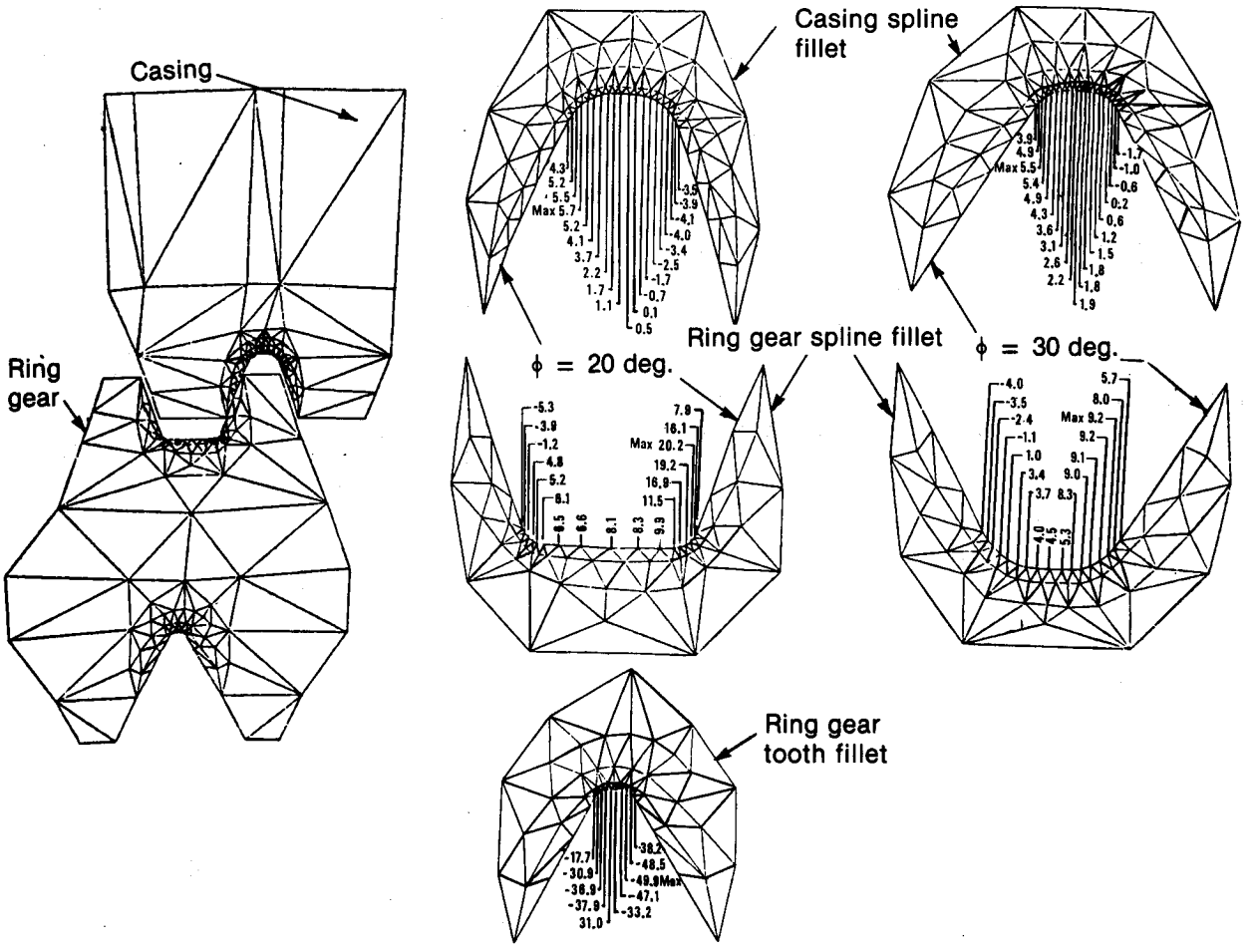

Fig. 5 Stress analysis F. E. model and fillet stress distribution.

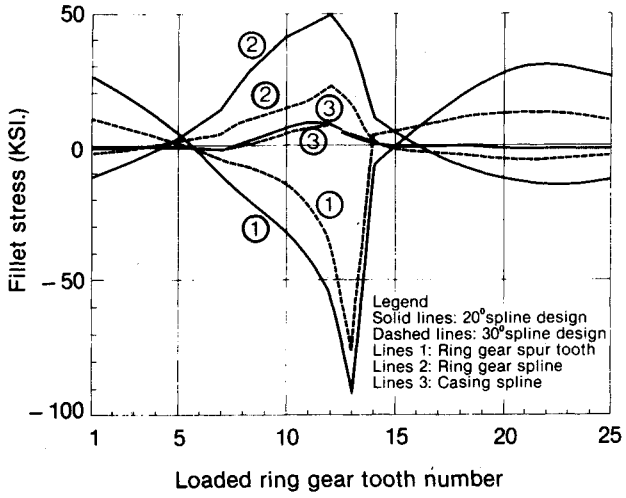

Fig. 6 Fillet stresses vs planet load position.

planet load. This takes less computer resources than refining the full model and running it for one planet load position.

The above calculations assume that the load sharing between the planets is equal. The dynamics of the system would in practice cause unequal load sharing. The loads and stresses along the face width of the gears will not also be uniform because of the misalignment at the teeth meshes. The extent of this misalignment is difficult to calculate analytically. It depends on the flexibility of the different components, especially the carrier and the hydrodynamic fluid film between the planet bushing and the shaft. The analytical details are explained in Ref. 5. These effects are generally taken into account through experimentally derived factors using signals from strain gages mounted in the fillet along the face width of the internal gear tooth and the spline. A relative comparison of the signals from the strain gages at any instant would give a measure of the misalignment factor. The variation in the peak strains registered by any one of the gages as the different planets orbit would give a measure of the planet load-sharing factor.

Discussion of Results

The structural analysis of the second stage of a large PT6 turbo propeller gearbox was performed because of casing spline-wear problems in the field. The flexibility of the ring gear concentrates the reaction to the planet load in a limited number of splines. Figure 4 shows the distribution of the reaction in the different splines as well as the relative sliding for the 20- and 30-deg pressure angle spline designs. This distribution was found to be only slightly altered for different positions of the planet load. Increasing the spline pressure angle distributes the reaction over the splines differently and the peak spline load is increased slightly. More significantly, the pressure angle increase reduces the relative sliding between the spline teeth, which is an important parameter affecting spline wear.

Figure 6 shows the variation of the fillet stresses for different planet positions. The ring gear stresses are due to the flexing of the ring as well as the tooth bending. It is very difficult to determine the combined action of the tooth bending and rim flexing without the aid of the finite-element method. When the spline fillets located on the outer surface of the ring gear register tensile stresses, the internal teeth fillets show compressive stresses due to rim flexing. The magnitude of the peak spline fillet stress is also relatively lower because of the load sharing between the splines. In contrast, all of the planet load is applied on one ring gear internal tooth at a certain instant thus generating higher peak stress. The casing spline fillet stresses are only due to spline tooth bending, shear, and compression. The flexing of the casing is set to zero by the fixity boundary conditions imposed on the casing outer radius. The high cycle fatigue evaluation of the design can be made using the stress variations after taking into account the effects of unequal planet load sharing and misalignment through the use of design factors as explained earlier.

Experimental Substantiations

The comparative analysis of the two designs with the 20- and the 30-deg pressure angles indicated significant reduction in the relative sliding with a small increase in the peak spline load. Wear tests conducted on coupons had indicated an exponential increase in wear due to increase in slip amplitude. Even if we assume that wear varies linearly with the product of peak spline load and the relative sliding, as shown in Fig. 4, we should expect a 50% reduction in the spline wear. Based on these findings, the pressure angle change was incorporated in the field engines. This eliminated the wear problem in the magnesium splines in current engines, giving confidence in the analysis.

Quantitative comparison of the fillet stresses with experimental strain-gage measurements is difficult. This is because even the miniature strain gages measure only average values of fillet stresses while the analysis predicts steep stress gradients. At the same time, the misalignment and dynamic effects included in the strain-gage measurements are not analytically predicted. As a result, only the form of variation of the stresses as the planets orbit can be compared between the analysis and measurement. Figure 7 shows the results of a typical strain-gage survey in an engine test with measurements made at the fillets of the ring gear spur tooth, spline, and casing spline. The spline pressure angle was 20 deg. The buildup of compressive stress in the ring gear spur tooth as the planet approaches the strain-gaged tooth and the sudden increase in the stress when the tooth is loaded can be seen in the analysis prediction in Fig. 6 and the experimental measurement in Fig. 7. The ring gear spline stresses are generally opposite in sign to the ring gear spur tooth stresses as can be expected due to ring flexing. The measured casing spline fillet stress is small and it alternates equally between tension and compression

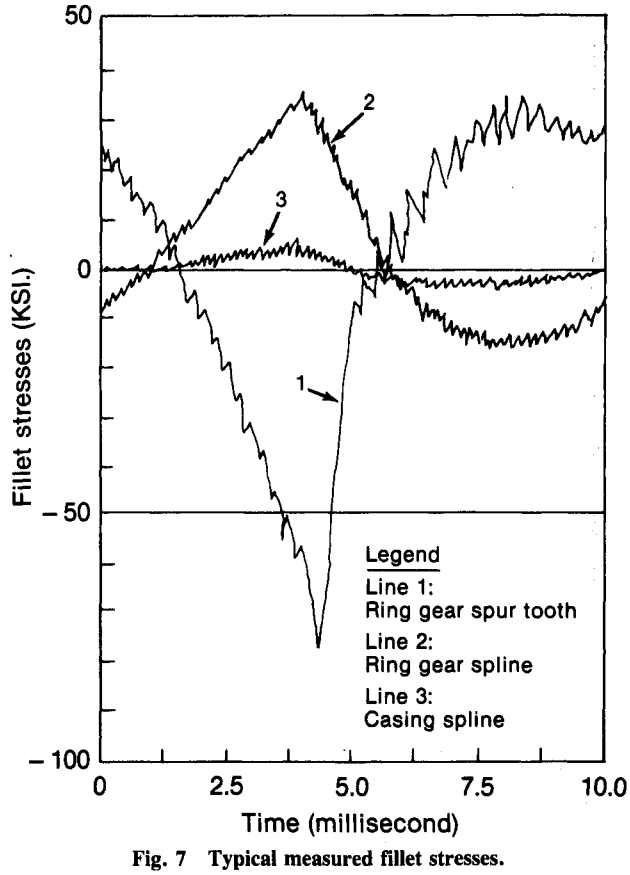

Fig. 7 Typical measured fillet stresses.

indicating flexing of the casing. The analysis prediction shows mostly tensile stresses. This is due to the assumed fixity boundary condition on the outer radius of the casing in the analysis. The flexing of the casing is prevented as a result. The qualitative comparison between the analysis and the measurement is thus considered to be good.

Conclusions

The ring gear in a planetary gearbox needs to be flexible due to dynamic considerations. However, this flexibility causes the reaction to the planet load to be concentrated in a limited number of external ring gear splines, when the casing is relatively fixed. Using automated iterative finite-element analysis, good prediction of spline load distribution is possible. The fillet stresses in the ring gear are due to a combination of ring flexing and tooth bending, and the finite-element analysis procedure takes into account these effects very well. The comparison with stresses measured using strain gages is found to be good. Three-dimensional effects, namely, misalignment and dynamic effects such as the planet load sharing, can be taken care of through experimentally derived design factors. Design modifications on the basis of predicted reduction in the relative sliding between the ring gear and the casing eliminated the spline wear problem in the gearboxes of the field engines.

Acknowledgment

The authors wish to thank Mr. Q. T. Trinh, Pratt and Whitney, Canada, for the analysis example included in the paper.

References

[1]Sundararajan, S., and Blanchette, R., "Finite-Element Contact Analysis of Ring Gear and Support," *Canadian Aeronautics and Space Journal*, Vol. 32, No. 2, June 1986, pp. 148–154.

[2]Brownridge, C., and Hollingworth, D., "Advanced Gearbox Technology in Small Turbo Propeller Engines," AGARD CP-369, April 1985.

[3]Chong, T., Suzuki, T., Aida, T., and Fujio, H., "Bending Stresses of Internal Spur Gear," *Bulletin of the JSME*, Vol. 25, No. 202, April 1982, pp. 679–686.

[4]Oda, S., and Kouitsu, H., "Root Stress of Thin-Rimmed Internal Spur Gear Supported with Pins," *International Journal of the JSME*, Vol. 30, No. 262, April 1987, pp. 646–652.

[5]Das, P. K., and Gupta, S. S., "An Analytical Method to Calculate Misalignment in the Journal Bearing of a Planetary Gear System," *Wear*, Vol. 61, June 2, 1980, pp. 143–156.